



Astrophysics (Planetary atmospheres)

High-resolution imaging spectroscopy of planetary atmospheres



Thérèse Encrenaz

LESIA, Observatoire de Paris, CNRS, UPMC, UPD, 92190 Meudon, France

ARTICLE INFO

Article history:

Received 6 February 2015

Accepted after revision 6 February 2015

Available online 30 March 2015

Handled by Vincent Courtillot

Keywords:

Mars

Venus

Jupiter

Planetary atmospheres

Infrared spectroscopy

ABSTRACT

Imaging spectroscopy at high resolution, in the infrared range, is a powerful tool for monitoring the behavior of minor species in planetary atmospheres and their evolution with latitude and longitude, season or local hour. Using the TEXES imaging spectrometer at the Infrared Telescope Facility (IRTF), this method has been applied for detecting and monitoring hydrogen peroxide and water vapor (using its proxy HDO) on Mars, then for monitoring sulfur dioxide and water (again using HDO) above the H_2SO_4 cloud deck ($z = 65$ km on Venus). Observations of Mars have shown that its atmosphere and climate are well reproduced by the Global Climatic Models. In contrast, strong spatio-temporal variations of SO_2 , observed above the Venus clouds, are not understood by the models. As a support of the forthcoming *Juno* space mission, a similar program has started on Jupiter to monitor its dynamics through 3-D maps of ammonia and phosphine.

© 2015 Académie des sciences. Published by Elsevier Masson SAS. All rights reserved.

1. Introduction

Over several decades, the atmospheres of planets (Venus, Mars, Jupiter and Saturn) have been monitored by numerous spacecraft (orbiters, landers and rovers in the case of Mars). Over the years, these missions have provided us with impressive datasets regarding the planetary atmospheric composition, thermal and cloud structure, and seasonal evolution. Still, ground-based imaging spectroscopy can provide important supplementary information. Indeed, ground-based instruments, being more sophisticated than space-borne instruments, can achieve a higher resolving power, essential for probing the tenuous molecular lines of the Martian atmosphere or the stratospheric emissions in the giant planets' atmospheres. In addition, the development of high-resolution imaging spectrometers now allows us to record instantaneous maps of minor species over the planetary disks, which

gives a unique opportunity for studying daily variations or transient phenomena.

Over the past ten years, we have been using the Texas Echelon Cross Échelle Spectrograph (TEXES), mounted at the 3-m Infrared Telescope Facility (IRTF) at Mauna Kea Observatory, to monitor the atmosphere of Mars and, more recently Venus and Jupiter. In the case of Mars, our first objective was to search for hydrogen peroxide H_2O_2 , a key molecule possibly responsible for the lack of organics at the Martian surface. After its detection in 2003, we have monitored its abundance (as well as HDO, simultaneously recorded as a proxy for water vapor) until 2014 as a function of latitude and season, and we have used these results to constrain global climatic photochemical models. Starting in 2012, we have used the same facility to monitor the behavior of sulfur dioxide and water vapor at the H_2SO_4 cloud-top ($z = 65$ km) and within the clouds (z about 60 km). In addition, in November 2011, we have used the Atacama Large Millimeter Array (ALMA) to obtain maps of SO , SO_2 , HDO and CO in the submillimeter range. These data probe the upper mesosphere of Venus, at an altitude

Email address: therese.encrenaz@obspm.fr.

of about 90 km. Finally, since February 2014, we have started a program on Jupiter to monitor two key tracers of its tropospheric dynamics, ammonia and phosphine, at different atmospheric levels, with pressures ranging from 0.1 bar to a few bars. This program will continue over the coming years as a support to the forthcoming *Juno* space mission, launched in August 2011 for an encounter of Jupiter in July 2016.

In this paper, we first present our results on the Martian atmosphere (Section 2), then on the Venus mesosphere using both ALMA (Section 3.1) and TEXES (Section 3.2). In Section 4, we briefly describe the Jupiter program and we discuss the perspectives of this work.

2. The atmosphere of Mars

Since the Mariner 9 and Viking era in the 1970s, the atmosphere of Mars has been repeatedly monitored by orbiters, landers and rovers. We now have a very good knowledge of the seasonal atmospheric evolution (chemical composition, thermal and cloud structure, dynamics, photochemistry). Global climatic models have been developed, especially at the Laboratoire de météorologie dynamique (LMD, Paris; Forget et al., 1999); they generally provide very good data fitting, at least below an altitude of about 50 km.

After the negative results of Viking regarding the presence of organics at the surface of Mars, the question was raised about the nature of the agent responsible for the oxidation of the surface. Hydrogen peroxide was suggested (Atreya and Gu, 1995; Clancy and Nair, 1996), although the amounts predicted by photochemical models appeared by far insufficient to destroy all organics (in particular those of meteoritical origin). Hydrogen peroxide was unsuccessfully searched for (Encrenaz et al., 2002; Krasnopolsky et al., 1997) until it was discovered through two ground-based experiments in 2003, first in the submillimeter range (Clancy et al., 2004), then by imaging spectroscopy (Encrenaz et al., 2004). The latter dataset is described below.

TEXES (Texas Echelon Cross-Échelle Spectrograph) is a high-resolution imaging spectrometer (Lacy et al., 2002), operating between 5 and 25 μm , that combines both very high spectral resolution ($R = 80,000$ at 8 μm in the high-resolution mode) and good spatial resolution (about 1 arcsec). At 8 μm , the 1.1×8 arcsec slit of the instrument, aligned along the north–south celestial axis, is moved from west to east with 0.5 arcsec steps. The size of Mars typically ranges between 6 and 15 arcsec. Two scans (north and south) are usually necessary to map the whole planet, which takes about 15 min. We choose an interval of about 7 cm^{-1} of bandwidth, centered at 1240 cm^{-1} , which contains several transitions of the strong ν_6 H_2O_2 band. In June 2003, the areocentric longitude was 206° (southern spring), corresponding to a high H_2O_2 content according to photochemical models. All H_2O_2 transitions were detected, together with CO_2 transitions (both strong and weak) and a couple of HDO transitions.

In order to map the H_2O_2 mixing ratio on the Martian disk, we selected a H_2O_2 doublet which brackets a weak CO_2 line at 1241.6 cm^{-1} , and we simply compute the ratio

of the line depths of the H_2O_2 transitions versus the CO_2 transitions. Radiative transfer calculations show that this line depth ratio is a very good indicator of the $\text{H}_2\text{O}_2/\text{CO}_2$ mixing ratio as it eliminates, to first-order, effects due to geometry and thermal structure. Fig. 1 shows the spectrum of the H_2O_2 doublet observed in June 2003 ($L_s = 206^\circ$) at the time of the first detection, and the first H_2O_2 map recorded for this season.

Since 2003, we have been observing H_2O_2 in November 2005, June 2008, October 2009, March 2014, and July 2014, to monitor its behavior as a function of time and season (Encrenaz et al., 2005, 2008, 2012a,b). As an example, Fig. 2 shows the H_2O_2 map retrieved with this method in March 2014 ($L_s = 96^\circ$), compared with the H_2O_2 map calculated using the LMD-GCM (Forget et al., 1999), including a photochemical model developed at LATMOS (Lefèvre et al., 2008). It can be seen that the H_2O_2 distribution over the disk is far from being uniform, and globally well fitted by the model. The disk-integrated H_2O_2 mixing ratio typically ranges between a few ppb and about 30 ppb. The conclusion of these observations is that the H_2O_2 behavior is well reproduced by the models. In particular, Fig. 3 shows the evolution of the H_2O_2 content as a function of L_s , compared with various photochemical models. It can be seen that the observations favor the LMD-IPSL model including heterogeneous chemistry on water ice grains (Encrenaz et al., 2012a,b, 2015a; Lefèvre et al., 2008). The same behavior is observed for the seasonal distribution of ozone on Mars, as well as in the terrestrial atmosphere, where the loss of polar ozone in the Earth's stratosphere has been explained by interactions between gaseous chemical species and ice cloud particles (Lefèvre et al., 2008).

Using weak HDO transitions in the $1237\text{--}1244 \text{ cm}^{-1}$ range, we have simultaneously retrieved maps of water vapor, using HDO as a tracer of H_2O . We made the assumption that D/H was constant over the Martian disk, with a value of 5.0 times the terrestrial value (Krasnopolsky et al., 1997). This is actually a first-order approximation, as theoretical calculations predict variations associated, in particular, with condensation (Montmessin et al., 2005). We assume a constant D/H value in the lack of precise measurements. The water vapor seasonal cycle is generally well understood on Mars since the Viking measurements and, more recently, the TES monitoring aboard the MGS orbiter (Smith, 2002, 2004), and maps of the water vapor content versus latitude and areocentric longitude are well represented by GCMs. However, no information has been acquired so far on two-dimensional maps of water vapor that would give, for any season, the H_2O distribution versus latitude and longitude, or versus latitude and local hour. This information requires imaging spectroscopic capabilities from some distance, as from the ground or Earth orbit, and has been obtained in the thermal regime for the first time with TEXES. In general, the agreement between the TEXES maps of HDO and H_2O maps predicted by the GCM is satisfactory. An example is shown in Fig. 4 for $L_s = 80^\circ$, just before the northern summer solstice, when water vapor is expected to be maximum. There is a very good agreement between the data and the model (Encrenaz et al., 2010).

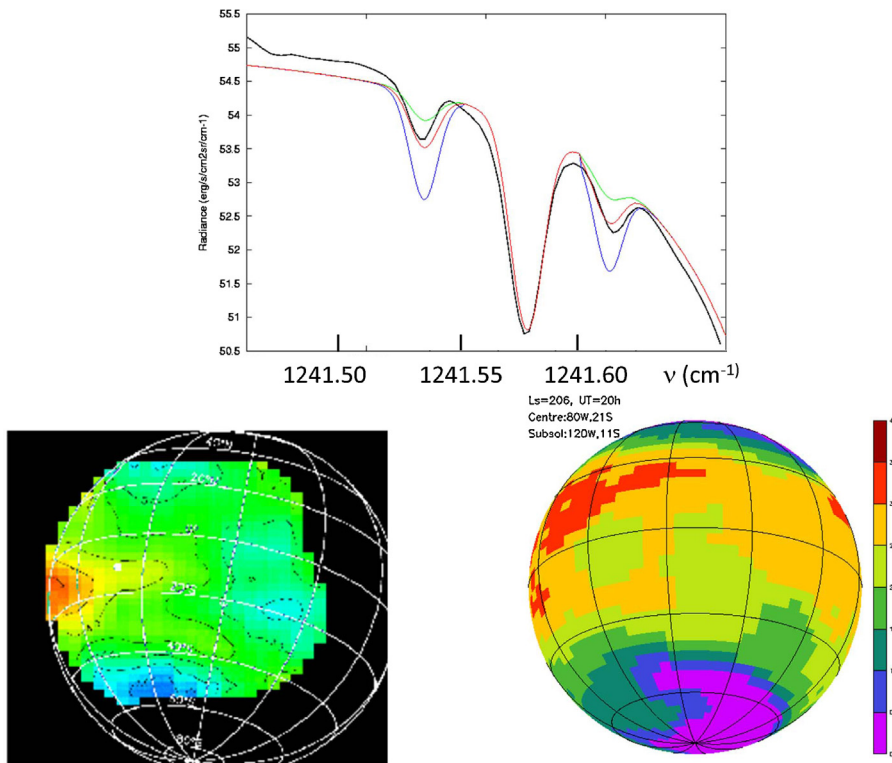


Fig. 1. (Color online.) Top: the TEXES spectrum of Mars (black curve) around 1241.6 cm^{-1} showing a doublet of H_2O_2 transitions (at 1241.53 and 1241.61 cm^{-1}) bracketing a CO_2 transition (at 1241.58 cm^{-1}). Line positions correspond to rest frequencies. Models: $[\text{H}_2\text{O}_2] = 20$ ppb (green), 40 ppb (red, best fit), and 80 ppb (blue). The spectrum is integrated in a region of the Martian disk where the H_2O_2 abundance is maximum. Bottom: left: map of the line depth ratio of $\text{H}_2\text{O}_2/\text{CO}_2$ retrieved from the TEXES data recorded in June, 2003 ($L_s = 206^\circ$). Right: GCM synthetic map of the H_2O_2 mixing ratio under the same observing conditions.

The figure is adapted from Encrenaz et al., 2004.

In summary, monitoring the Martian atmosphere using high-resolution ground-based imaging spectroscopy has allowed us to monitor the seasonal variations of hydrogen peroxide and water vapor, and to give indication for H_2O_2

photochemical models including heterogeneous chemistry. It has also confirmed that the GCM provides a very good understanding of the Martian climate in terms of chemical composition and thermal structure.

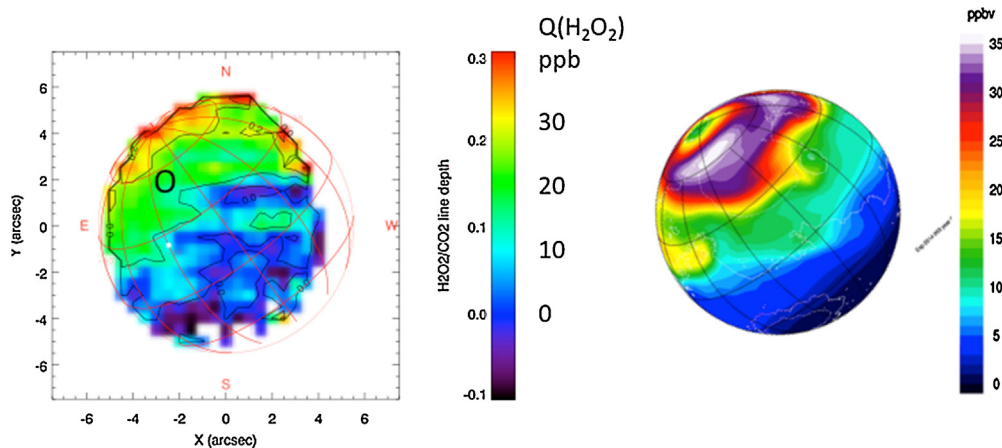


Fig. 2. (Color online.) Left: map of the line depth ratio of $\text{H}_2\text{O}_2/\text{CO}_2$ retrieved from the TEXES data recorded on 1 March 2014 ($L_s = 96^\circ$). Right: GCM synthetic map of the H_2O_2 mixing ratio under the same observing conditions. Note that the color scales of the two maps are different: the maximum mixing ratio of H_2O_2 is 35 ppbv in both cases.

The figure is adapted from Encrenaz et al. (2015a).

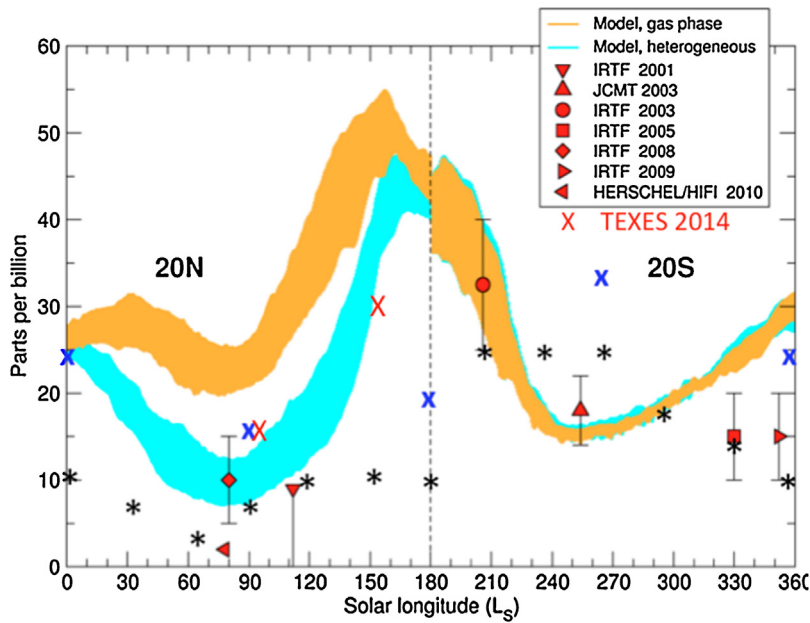


Fig. 3. (Color online.) The seasonal cycle of the H_2O_2 mixing ratio on Mars. TEXES observations refer to 20 N latitudes for $L_s = 0-180^\circ$ and to 20S latitudes for $L_s = 180-360^\circ$, in order to match as best as possible the observing conditions induced by the axial tip of the planet. Submillimeter observations refer to the entire disk. GCM simulations ignore (yellow) or include (light blue) heterogeneous chemistry. Other 1-D photochemical models are shown for comparison (black stars: Krasnopolsky, 2009; blue crosses: Moudren, 2007). The Herschel point at $L_s = 77^\circ$ corresponds to an upper limit. The two red crosses correspond to the TEXES 2014 observations. The figure is adapted from Lefèvre et al. (2008).

3. The atmosphere of Venus

While both Mars and Venus have in common a CO_2 -dominated atmosphere, with N_2 , Ar, CO, H_2O as minor species, the atmosphere of Venus presents, as compared to the Martian atmosphere, an extreme case with very high surface pressure (90 bar) and temperature (730 K). In addition, sulfur (most likely outgassed from the interior) plays a major role in the photochemistry and dynamics of Venus. The surface of Venus is hidden by an opaque cloud

deck, rich in sulfuric acid, extending to altitudes of about 50–65 km.

In contrast with the case of Mars, the atmosphere of Venus is far from being understood in terms of vertical transport and dynamics. Even the mass budget of sulfur is not understood. Indeed, both SO_2 and H_2O are relatively abundant (150 ppm and 30 ppm respectively) in the lower troposphere, below the cloud deck (Bézar and de Bergh, 2007). Above the clouds, these abundances drop down to about 100 ppb and 1 ppm, respectively (Marcq et al., 2011;

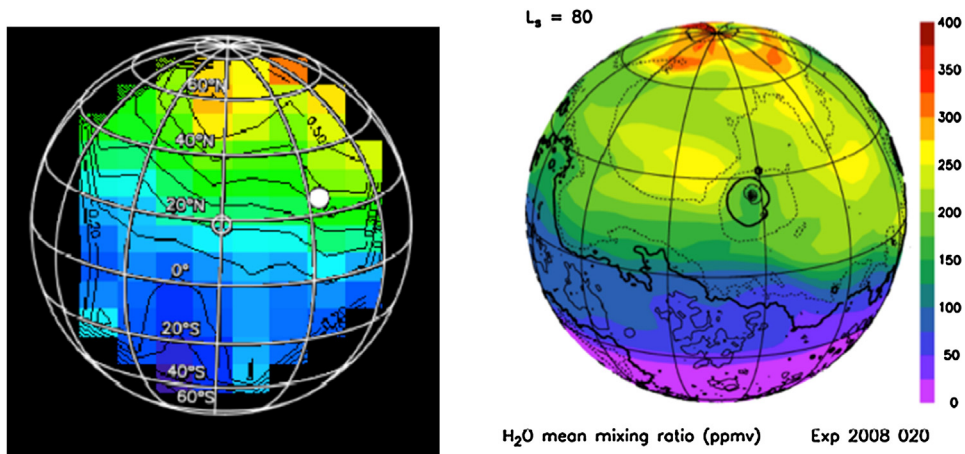


Fig. 4. (Color online.) Comparison of TEXES maps and GCM simulations for the June 2008 data set ($L_s = 80^\circ$). The water vapor mixing ratio is indicated (250 ppm at 30N–50N). The figure is taken from Encrenaz et al. (2010).

Zasova et al., 1993). Assuming that most of water combines with SO_2 to form H_2SO_4 , only one fifth of the total SO_2 content is used in this process. So in which form is the remaining sulfur? Most likely in the form of aerosols, but their exact nature – and thus their optical and radiative properties – is not known. Above the cloud deck, another surprising result has been found. In the lower mesosphere, the SO_2 mixing ratio is known to decrease with altitude, down to a few ppb above the clouds (Belyaev et al., 2012). Then, it increases again in the upper mesosphere, at a level of about 90 km, where SO and SO_2 have both been detected in the submillimeter range, at a level of a few tens of ppb (Sandor et al., 2010, 2012). Thus, a second reservoir, probably also made of sulfur aerosols, must be present at these altitudes.

Since 2011, we have been observing water and sulfur species on Venus on different occasions and at different altitudes. In November 2011, we have used the Atacama Large Millimeter Array (ALMA) facility to obtain submillimeter maps of minor species in the upper atmosphere, at an altitude of about 90 km. In January and October 2012, we have used TEXES at IRTF to study the spatio-temporal variations of SO_2 and H_2O (through its proxy HDO) at the cloud-top and within the clouds. These observations have shown evidence of strong spatial and temporal variations of the sulfur species, both at the cloud-top and in the upper

mesosphere. These variations are presently not understood by the photochemical or dynamical models.

3.1. ALMA observations the upper mesosphere

We observed Venus with ALMA in November 2011 during Cycle 0 (Early Science Phase). Alma is an international facility that, using a set of 66 antennas of 7 to 12-m diameter, provides high-resolution heterodyne spectroscopy ($R > 10^6$) in spectral atmospheric windows covering the whole millimeter–submillimeter range (80–800 GHz, corresponding to wavelengths of 500 μm –3.7 mm). At the time of our observations, 16 antennas of 12-m diameter were available. Venus was about 11 arcsec in diameter, and we obtained maps with a spatial resolution of about 2 arcsec. We chose a set of transitions near 345 GHz and we observed simultaneously CO at 345.796 GHz, HDO at 335.955 GHz, SO at 346.528 GHz, and SO_2 at 346.620 GHz. Four observing runs of 30 min each were recorded on 14, 15, 26 and 27 November 2011, successively. The preliminary results are presented in Encrenaz et al. (2015a).

Fig. 5 shows the variations of SO, SO_2 and HDO on 14 and 15 November. The SO map is of best quality because, although SO is less abundant than SO_2 , the SO transition is intrinsically much stronger. All three species show significant variations over the disk and over a

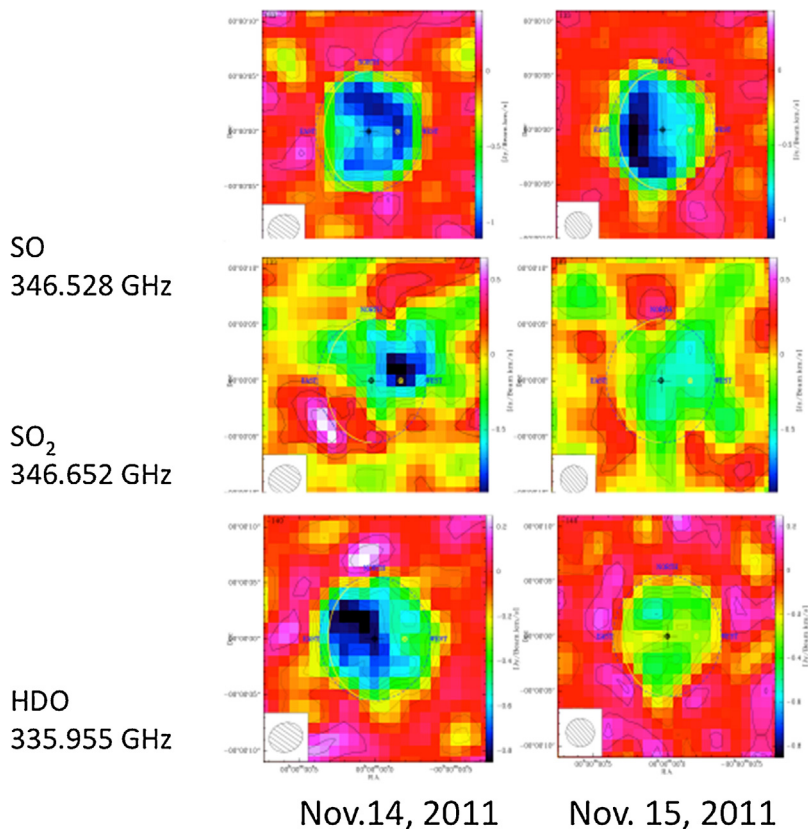


Fig. 5. (Color online.) Maps of the intensities of SO (346.528 GHz, top), SO_2 (346.652 GHz, middle) and HDO (335.955 GHz, bottom) transitions recorded with ALMA on November 14 (left) and 15 (right), 2011 with the ALMA facility. The submillimeter radiation probes the upper stratosphere ($z = 90$ km). All species show significant spatial and temporal variations over a timescale of a day. The figure is adapted from Encrenaz et al. (2015b).

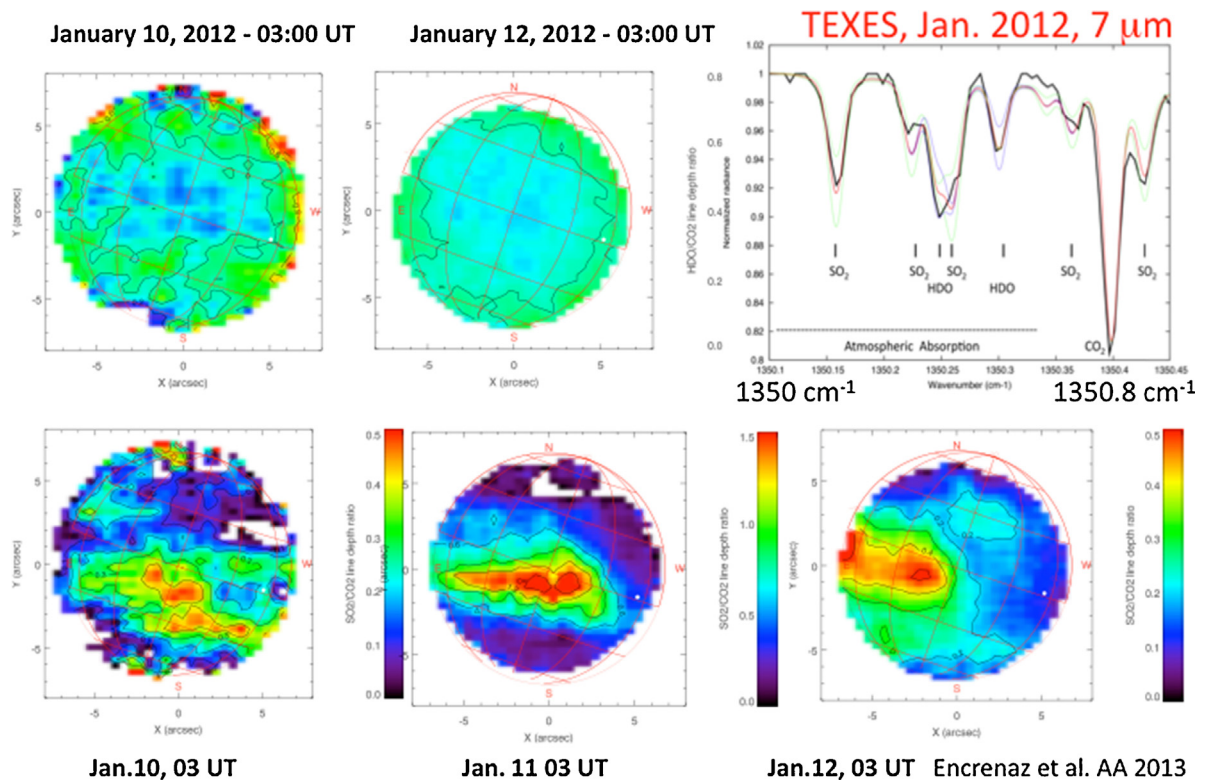


Fig. 6. Upper left: maps of HDO recorded at the cloud-top of Venus on January 10 and 12, 2012. The maps show no significant variation over space and time. Upper right: the spectrum of Venus extracted around 1350 cm^{-1} in a region of maximum SO_2 signal, showing transitions of SO_2 , HDO and CO_2 . Bottom: maps of SO_2 at the cloud-top recorded on January 10, 11 and 12, 2012. Strong variations are observed over the disk and over a timescale of one day. The figure is adapted from Encrenaz et al. (2012b, 2013).

timescale of a day. In the case of HDO, the variations could be associated with fluctuations of the mesospheric temperature; in the case of the sulfur species, the origin of these variations is unknown.

We have also used the disk-integrated spectra of SO , SO_2 and HDO on 14 November to infer their mean mixing ratios and vertical distributions. Both sulfur species show a cut-off below the altitude level of 88 km, and mixing ratios of 8 ppb and 12 ppb, respectively, above this level. The HDO vertical distribution, in contrast, is well fitted with a constant H_2O mixing ratio of about 2.5 ppm, assuming a D/H ratio of 200 times the terrestrial value in the upper mesosphere (Fedorova et al., 2008).

3.2. TEXES observations of the lower mesosphere

Fig. 6 summarizes the observations of SO_2 and HDO obtained in January 2012 over a timescale of 3 days, at the cloud-top of Venus ($z=65\text{ km}$), using high-resolution spectra around 1350 cm^{-1} ($\lambda=7.4\text{ }\mu\text{m}$). It can be seen that SO_2 shows strong spatial variations over the disk, and significant changes within a day; in contrast, the water distribution is much more uniform and constant with time. The maximum mixing ratio of SO_2 is about 100 ppb, and the H_2O mixing ratio, constant over the disk, is about 1.5 ppm (Encrenaz et al., 2012).

Subsequent observations of SO_2 and HDO, in October 2012, February 2014 and July 2014, have confirmed the

high variability of SO_2 (over a timescale as short as 2 h) and the more or less constant distribution of H_2O over the disk and with time (Encrenaz et al., 2013, 2014a, b, c). In addition, spectra of SO_2 have been obtained at $19\text{ }\mu\text{m}$, where the radiation comes from within the clouds, a few kilometres below the cloud-top. Vertical distributions of SO_2 and HDO have been retrieved in areas of maximum abundances. Best fits are obtained with a cut-off in the vertical distribution of SO_2 at a level located a few kilometres above the cloud-top. In contrast, the HDO spectra are well fitted with a water vertical distribution constant with altitude. Another interesting result was a drop by a factor 3 of the disk-integrated mixing ratio of SO_2 at the cloud-top in February 2014, as compared with the three other runs (Encrenaz et al., 2014b). All these results are globally consistent with *Venus Express* results taken by SPICAV and SOIR (Belyaev et al., 2012; Marcq et al., 2011), but are presently unexplained by theoretical models.

It is interesting to compare the TEXES and ALMA data, in spite of the time difference (one month) between the two data sets. The SO_2 vertical distribution shows a strong depletion a few kilometres above the clouds ($z=67\text{--}70\text{ km}$), then increases again above 90 km. In contrast, the H_2O vertical distribution appears to be constant in the mesosphere. The SO_2 spatial distribution is patchy and changes over short timescales, both in the lower and upper mesosphere. The H_2O distribution is constant with space and time in the lower mesosphere; at higher altitudes

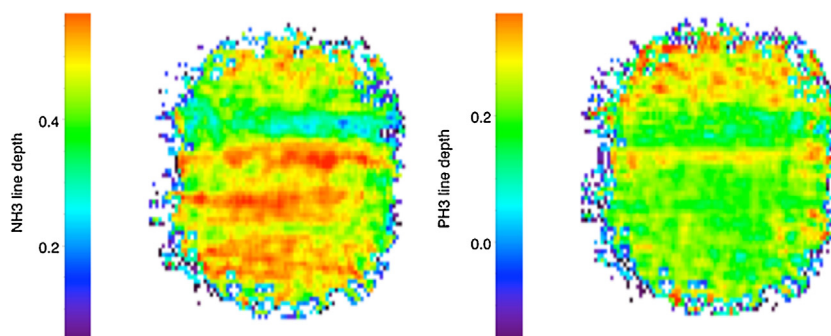


Fig. 7. (Color online.) Maps of NH_3 and PH_3 transitions recorded at 1134.0 cm^{-1} and 1133.2 cm^{-1} respectively, probing the 0.5-bar pressure level near the ammonia condensation level. The two maps show significant differences, associated with different transport mechanisms. The PH_3 shows a trend for enrichment toward high northern latitudes, also observed at other altitude levels. The figure is adapted from Encrenaz et al. (2014c).

where water condensation can take place, the HDO variations might be associated with temperature fluctuations.

4. The future: monitoring the dynamics of Jupiter in support of the *Juno* mission

In July 2016, the *Juno* space mission, launched by NASA in August 2011, will encounter Jupiter. One of its main objectives is the measurement of the O/H ratio in the deep interior of the planet, a key measurement for understanding the nature of the planetesimals that formed the planet (Atreya et al., 1999). This measurement will be made in the radio range where water has a major contribution to the continuum spectrum (Janssen et al., 2005). However, other minor species (NH_3 , PH_3 , H_2S ...) also have contributions in this spectral range; in particular, ammonia is a major radio absorber.

Ammonia and phosphine are both tracers of Jovian dynamics. PH_3 is a disequilibrium species that is not expected to be observed in the Jovian spectra, as it should react with H_2O in the deep troposphere to form P_4O_6 . Its presence in the upper troposphere is due to vertical motions that carry the molecule upward on timescales shorter than the destruction lifetime of the molecule (Lewis, 1997). The presence of NH_3 , in contrast, is predicted by thermo-chemical models. Its abundance is constrained by reactions with H_2O and H_2S to form NH_4OH and NH_4SH clouds at about 2 bar, then by NH_3 condensation above the 0.5 bar level (Atreya, 1986). Both ammonia and phosphine are thus tracers of Jovian dynamics; it is important to measure their abundances in the troposphere of Jupiter, and to monitor their possible temporal variations.

In February 2014, we have started an observing program to monitor the abundances of NH_3 and PH_3 at different atmospheric levels of the Jovian troposphere (with pressure levels ranging from 0.1 bar to a few bars). Using the same technique as that developed for our Mars and Venus observations, we have mapped the Jovian disk in three different spectral ranges probing different pressure levels: $4.64\ \mu\text{m}$ ($P = 3\text{--}5$ bar); $8.83\ \mu\text{m}$ ($P = 0.3\text{--}0.5$ bar); $10.47\ \mu\text{m}$ ($P = 0.1\text{--}0.3$ bar). Preliminary results

are given in Fig. 7, which shows maps of the line depths of two specific transitions of NH_3 and PH_3 at the 0.3–0.5 bar pressure level. It can be seen that both maps are distinctly different, illustrating that both molecules are sensitive to different dynamical mechanisms; in addition, the PH_3 abundance seems to be enhanced at high northern latitudes, a trend that is also observed at other pressure levels (Encrenaz et al., 2015b). This work will be pursued in 2015 and beyond, with the objective of mapping the abundances of these two species as a function of time, longitude, and latitude at the time of the *Juno* mission.

Acknowledgements

This is an invited contribution to the special issue “Invited contributions of 2014 geoscience laureates of the French Academy of Sciences”. It has been reviewed by Françoise Combes and Editor Vincent Courtillot. The author is most grateful to T. Greathouse, M. Richter and J. Lacy, who have developed and are operating the TEXES instrument, and to A. Tokunaga, Director of IRTF, for the support of the IRTF staff. She is also most grateful to R. Moreno and to the Alma Regional Center in Grenoble for the reduction of the ALMA data. She wants to thank her friends and colleagues from LESIA (B. Bézard, P. Drossart, T. Fouchet, E. Lellouch, R. Moreno, T. Widemann) and from IPSL (F. Forget, F. Lefèvre, F. Montmessin) who have participated in these programs. This work was supported by the Programme national de planétologie, CNRS/INSU.

References

- Atreya, S.K., 1986. Atmospheres and ionospheres of giant planets and their satellites. Springer-Verlag.
- Atreya, S.K., Gu, Z.G., 1995. Photochemistry and stability of the atmosphere of Mars. *Adv. Space Res.* 16 (6), 57–68.
- Atreya, S.K., Wong, M.H., Owen, T.C., Mahaffy, P.R., Niemann, H.B., de Pater, I., Drossart, P., Encrenaz, T., 1999. A comparison of the atmospheres of Jupiter and Saturn: deep atmospheric composition, cloud structure, vertical mixing, and origin. *Plan. Space Sci.* 47, 1243–1262.
- Belyaev, D., Montmessin, F., Bertaux, J.-L., et al., 2012. Sulphur oxides in Venus mesosphere detected from SPICAV-SOIR VEX solar occultation. *Icarus* 217, 740–751.
- Bézard, B., de Bergh, C., 2007. Composition of the atmosphere of Venus below the clouds. *J. Geophys. Res.* 112, E04S07.

- Clancy, R.T., Nair, H., 1996. Annual (aphelion-perihelion) cycles in the photochemical behavior of the global Mars atmosphere. *J. Geophys. Res.* 101, 12785–12790.
- Clancy, R.T., Sandor, B.J., Moriarty-Schieven, G.H., 2004. A measurement of the 365 GHz line of Mars atmospheric H₂O₂. *Icarus* 168, 116–121.
- Encrenaz, T., Greathouse, T.K., Bézard, B., et al., 2002. A stringent upper limit of the H₂O₂ abundance in the Martian atmosphere. *Astron. Astrophys.* 396, 1037–1044.
- Encrenaz, T., Bézard, B., Greathouse, et al., 2004. Hydrogen peroxide on Mars: evidence for spatial and temporal variations. *Icarus* 170, 424–429.
- Encrenaz, T., Bézard, B., Owen, T., et al., 2005. Infra-red imaging spectroscopy of Mars: H₂O mapping and determination of CO₂ isotopic ratios. *Icarus* 179, 43–54.
- Encrenaz, T., Greathouse, T.K., Richter, M.J., et al., 2008. Simultaneous mapping of H₂O and H₂O₂ on Mars from high-resolution imaging spectroscopy. *Icarus* 195, 547–555.
- Encrenaz, T., Greathouse, T.K., Bézard, B., Fouchet, T., Lefèvre, F., et al., 2010. Water vapor map of Mars near summer solstice using ground-based infrared spectroscopy. *Astron. Astrophys.* 520, A33.
- Encrenaz, T., Greathouse, T.K., Lefèvre, F., Atreya, S.K., 2012. Hydrogen peroxide on Mars: observations, interpretation and future plans. *Plan. Space Sci.* 68, 3–17.
- Encrenaz, T., Greathouse, T.K., Roe, H., 2012b. HDO and SO₂ thermal mapping on Venus: evidence for strong SO₂ variability. *Astron. Astrophys.* 543, A153.
- Encrenaz, T., Greathouse, T.K., Richter, M.J., Lacy, J., Widemann, T., Bézard, B., et al., 2013. HDO and SO₂ thermal mapping on Venus, II. The SO₂ spatial distribution above and within the clouds. *Astron. Astrophys.* 559, A65.
- Encrenaz, T., Greathouse, T.K., Lefèvre, F., Richter, M.J., Lacy, J.H., Fouchet, T., 2014a. H₂O₂, H₂O and HDO thermal mapping on Mars using TEXES/IRTF and EXES/SOFIA. In: Communication presented at the EPSC Conference, Cascais (Portugal), September.
- Encrenaz, T., Greathouse, Richter, M.J., Lacy, J.H., Widemann, T., Bézard, B., 2014b. Imaging spectroscopy of Venus in the thermal infrared. In: Communication presented at the EPSC Conference, Cascais (Portugal), September.
- Encrenaz, T., Greathouse, Drossart, P., Fouchet, T., Janssen, M., Gulkis, S., 2014c. Monitoring Jovian dynamics using maps of NH₃ and PH₃. In: Communication presented at the EPSC Conference, Cascais (Portugal), September.
- Encrenaz, T., Greathouse, T.K., Lefèvre, F., Richter, M.J., Lacy, J.H., Fouchet, T., 2015a. H₂O₂. Seasonal variations of hydrogen peroxide and water vapor on Mars: more indication for heterogeneous chemistry. *Astron. Astrophys.* (under review).
- Encrenaz, T., Moreno, R., Moullet, A., Lellouch, E., Fouchet, T., 2015b. Submillimeter mapping of minor atmospheric species on Venus with ALMA. *Plan. Space Sci.* (under review).
- Fedorova, A., Korablev, O., Vandaele, A.-C., Bertaux, J.-L., Belyaev, D., Mahieux, A., Neefs, E., Wilquet, W.V., Drummond, R., Montmessin, F., Villard, E., 2008. HDO and H₂O vertical distributions and isotopic ratio in the Venus mesosphere by Solar Occultation at Infrared spectrometer on board Venus Express. *J. Geophys. Res.* 113, E12 CitelD E00B22.
- Forget, F., Hourdin, F., Fournier, R., 1999. Improved circulation models of the Martian atmosphere from the surface and above 80 km. *J. Geophys. Res.* 104, 24155–24176.
- Janssen, M.A., Hofstadter, M.D., Gulkis, S., Ingersoll, A.P., Allison, M., Bolton, S.J., Levin, S.M., Kamp, L.W., 2005. Microwave remote sensing of Jupiter's atmosphere from an orbiting spacecraft. *Icarus* 173, 447–453.
- Krasnopolsky, V.A., 2009. Seasonal variations of photochemical tracers at low and middle latitudes on Mars: Observations and models. *Icarus* 201, 564–569.
- Krasnopolsky, V.A., Bjoraker, G.L., Mumma, M.J., Jennings, D.E., 1997. High-resolution spectroscopy of Mars at 3.7 and 8 μm: a sensitive search of H₂O₂, H₂CO, HCl and CH₄, and detection of HDO. *J. Geophys. Res.* 102, 6525–6534.
- Lacy, J.H., Richter, M.J., Greathouse, T.K., et al., 2002. TEXES: A sensitive high-resolution grating spectrograph for the mid-infrared. *Pub. Astron. Soc. Pac.* 114, 153–168.
- Lefèvre, F., Bertaux, J.-L., Clancy, R.T., et al., 2008. Heterogeneous chemistry in the atmosphere of Mars. *Nature* 454, 971–975.
- Lewis, J.S., 1997. Physics and chemistry of the solar system. Academic Press.
- Marcq, E., Belyaev, D., Montmessin, F., Fedorova, A., Bertaux, J.-L., Vandaele, A.C., Neefs, E.A., 2011. Investigation of the SO₂ content of the venusian mesosphere using SPICAV-UV in nadir mode. *Icarus* 218, 58–69.
- Montmessin, F., Fouchet, T., Forget, F., 2005. Modeling the annual cycle of HDO in the Martian atmosphere. *J. Geophys. Res.* 110, E3 (CitelD 03006).
- Moudden, Y., 2007. Simulated seasonal variations of hydrogen peroxide in the atmosphere of Mars. *Plan. Space Sci.* 55, 2137–2143.
- Sandor, B.J., Clancy, R.T., Moriarty-Schieven, G., Mills, Franklin, P., 2010. Sulfur chemistry in the Venus mesosphere from SO₂ and SO microwave spectra. *Icarus* 208, 49–60.
- Sandor, B.J., Clancy, R.T., Moriarty-Schieven, G., 2012. Upper limits for H₂SO₄ in the mesosphere of Venus. *Icarus* 217, 839–844.
- Smith, M.D., 2002. The annual cycle of water vapor on Mars as observed by the thermal emission spectrometer. *J. Geophys. Res.* 107, 5115, <http://dx.doi.org/10.1029/2001JE001522>.
- Smith, M.D., 2004. Interannual variability in TES observations of Mars during 1999–2003. *Icarus* 167, 148–165.
- Zasova, L.V., Moroz, V.I., Esposito, L.W., Na, C.Y., 1993. SO₂ in the middle atmosphere of Venus: IR measurements from Venera-15 and comparison to UV data. *Icarus* 105, 92–109.